Since January 2020 Elsevier has created a COVID-19 resource centre with free information in English and Mandarin on the novel coronavirus COVID-19. The COVID-19 resource centre is hosted on Elsevier Connect, the company's public news and information website.

Virology 408 (2010) 241–252

Contents lists available at ScienceDirect

Virology

journal homepage: www.elsevier.com/locate/yviro

Identification of aromatic amino acid residues in conserved region VI of the large polymerase of vesicular stomatitis virus is essential for both guanine-N-7 and ribose 2'-O methyltransferases

Xiaodong Zhang [a,b], Yongwei Wei [b], Yuanmei Ma [b], Songhua Hu [a], Jianrong Li [b,c,*]

[a] College of Animal Science, Zhejiang University, Hangzhou, Zhejiang, China
[b] Department of Food Science and Technology, College of Food, Agricultural and Environmental Sciences, The Ohio State University, Columbus, OH, USA
[c] Division of Environmental Health Sciences, College of Public Health, The Ohio State University, Columbus, OH, USA

ARTICLE INFO

Article history:
Received 9 July 2010
Returned to author for revision
23 August 2010
Accepted 17 September 2010
Available online 18 October 2010

Keywords:
mRNA cap methyltransferase
Vesicular stomatitis virus
RNA methylation, replication
and gene expression

ABSTRACT

Non-segmented negative-sense RNA viruses possess a unique mechanism for mRNA cap methylation. For vesicular stomatitis virus, conserved region VI in the large (L) polymerase protein catalyzes both guanine-N-7 (G-N-7) and ribose 2'-O (2'-O) methyltransferases, and the two methylases share a binding site for the methyl donor S-adenosyl-l-methionine. Unlike conventional mRNA cap methylation, the 2'-O methylation of VSV precedes subsequent G-N-7 methylation. In this study, we found that individual alanine substitutions in two conserved aromatic residues (Y1650 and F1691) in region VI of L protein abolished both G-N-7 and 2'-O methylation. However, replacement of one aromatic residue with another aromatic residue did not significantly affect the methyltransferase activities. Our studies provide genetic and biochemical evidence that conserved aromatic residues in region VI of L protein essential for both G-N-7 and 2'-O methylations. In combination with the structural prediction, our results suggest that these aromatic residues may participate in RNA recognition.

Introduction

Eukaryotic mRNAs possess at their 5′ terminus a 7^{m}GpppN cap structure that is essential for mRNA stability and efficient translation (Furuichi et al., 1977; Furuichi and Shatkin, 2000). Formation of the cap structure usually requires four enzymatic reactions. First, an RNA triphosphatase hydrolyses the 5' triphosphate end of the nascent mRNA to yield a diphosphate (5' ppN). Second, the diphosphate RNA end is capped with GMP by an RNA guanylyltransferase via a covalent enzyme-GMP intermediate to yield the GpppN cap structure. Third, the N-7 position of guanine cap is methylated by a guanine-N-7 (G-N-7) MTase to yield 7^{m}GpppN. Finally, for some eukaryotic mRNA, the cap structure can be further methylated by a ribose-2′-O (2′-O) MTase to yield 7^{m}GpppN^{m}. The mRNA capping and methylation reactions are conserved among all eukaryotes (Shuman and Schwer, 1995; Furuichi and Shatkin, 2000; Shuman, 2001). In this conventional cap methylation reaction, two methylase activities are carried out by separate enzymes, each containing its own catalytic site and the binding site for the methyl donor, *S*-adenosylmethionine (SAM).

The non-segmented negative-sense (NNS) RNA viruses include a wide range of significant animal, human, and plant pathogens. The NNS RNA viruses are classified into four families: the *Rhabdoviridae*, as exemplified by vesicular stomatitis virus (VSV) and rabies virus; the *Paramyxoviridae*, as exemplified by human respiratory syncytial virus (RSV) and human parainfluenza virus type 3 (PIV3); the *Filoviridae*, as exemplified by Ebola and Marburg viruses; the *Bornaviridae*, as exemplified by Borna disease virus (BDV). With the exception of *Bornaviridae*, NNS RNA viruses typically replicate in the cytoplasm. These viruses share a common strategy for gene expression and replication (Rose and Whitt, 2001; Whelan et al., 2004). For many years, VSV has been used as a model to study the replication and gene expression of NNS RNA viruses. The viral genomic RNA is tightly encapsidated by the nucleocapsid (N) protein, forming the N-RNA complex that serves as a functional template for replication and transcription, which carried out by RNA-dependent RNA polymerase (RdRP). The viral RdRp is comprised of the catalytic subunit large (L) polymerase protein and the accessory phosphoprotein (P) (Emerson and Wagner, 1972; Emerson and Yu, 1975). During transcription, the RdRp complex transcribes the viral genome into five mRNAs in a sequential and gradient manner, such that 3′ proximal genes are transcribed more abundantly than 3′ distal genes (Abraham and Banerjee, 1976; Ball and White, 1976; Villarreal et al., 1976). These mRNAs are capped and methylated at the 5′ end and polyadenylated at the 3′ end (Iverson and Rose, 1981). During replication, it yields

* Corresponding author. Department of Food Science and Technology, College of Food, Agricultural and Environmental Sciences, Division of Environmental Health Sciences, College of Public Health, The Ohio State University, 233 Parker Food Science Building, 2015 Fyffe Road, Columbus, OH 43210, USA. Fax: +1 614 292 0218.
E-mail address: li.926@osu.edu (J. Li).

0042-6822/$ – see front matter © 2010 Elsevier Inc. All rights reserved.
doi:10.1016/j.virol.2010.09.017

full-length antigenomic RNA, which in turn results in the synthesis of genomic RNA. How polymerase complex controls these two distinct RNA synthesis is still poorly understood.

The VSV L protein is a 241-kDa multifunctional protein. Structure has not been determined for any of portion of L protein within NNS RNA viruses. In addition to the polymerase function, the L protein possesses all the enzymatic activities for mRNA processing such as capping, methylation and polyadenylation (Abraham et al., 1975; Moyer, 1981; Hercyk et al., 1988; Poch et al., 1990; Li et al., 2005, 2006, 2008, 2009; Galloway and Wertz, 2008; Ogino et al., 2010). In recent years, many breakthroughs have been made in VSV mRNA processing. These discoveries were facilitated by the ability of purified VSV to synthesize RNA in vitro (Baltimore et al., 1970) and the ability of highly purified L protein to modify short virus-specific mRNA in vitro (Ogino and Banerjee, 2007; Li et al., 2008; Rahmeh et al., 2009). Recent studies revealed that the mechanism of mRNA cap formation in VSV is distinct from that of all other known capping reactions. Specifically, capping of VSV mRNA is achieved by a novel polyribonucelotidyltransferase (PRNTase) which transfers a monophosphate RNA onto a GDP acceptor through a covalent L-RNA intermediate (Ogino and Banerjee, 2007; Li et al., 2008; Ogino et al., 2010). However, all other known capping reactions are catalyzed by a RNA guanylyltransferase, which transfers GMP derived from GTP onto a diphosphate acceptor RNA (Furuichi and Shatkin, 2000). Previously, we demonstrated that a new motif, GxxT[n]HR, in conserved region V (CRV) of the L protein is essential for PRNTase activity (Li et al., 2008). Mutation to this motif resulted in the synthesis of short abortive transcripts that lack a cap structure (Li et al., 2008). A biochemical study showed that it is the H residue in GxxT[n]HR motif involved in the formation of the covalent L-RNA intermediate (Ogino et al., 2010). In addition, it was shown that mRNA capping reaction of Chandipura virus, another member within the family *Rhabdoviridae,* utilizes the same mechanism (Ogino and Banerjee, 2010). Whether this unconventional mechanism is conserved in other families of NNS RNA viruses is not known.

Like the unconventional capping mechanism, methylation of the VSV mRNA cap structure is also unique. Specifically, the G-N-7 and 2'-O methylations of VSV mRNA are accomplished by a single protein: the conserved domain VI of the L protein (Grdzelishvili et al., 2005; Li et al., 2005, 2006, 2007, 2008; Galloway and Wertz, 2008; Galloway et al., 2008; Rahmeh et al., 2009). Sequence alignment and structure prediction identified a putative 2'-O MTase in conserved region VI of the L protein (Bujnicki and Rychlewski, 2002; Ferron et al., 2002). Alterations to the MTase catalytic motif (K-D-K-E) in conserved domain VI of VSV L protein abolished both G-N-7 and 2'-O methylations, suggesting that a single active site is essential for both methylase activities (Li et al., 2005). This is in contrast to all other known MTases, in which the two activities are catalyzed by either separate proteins (Shuman and Schwer, 1995; Furuichi and Shatkin, 2000) or two different regions in one protein (Reinisch et al., 2000). Interestingly, substitutions to the SAM binding site of VSV MTase disrupted methylation at the guanine-N-7 (G-N-7) position or at both the G-N-7 and ribose-2'-O (2'-O) positions of the mRNA cap, suggesting that the two methylase activities share one SAM binding site, and methylation of the G-N-7 position is not required for 2'-O methylation (Li et al., 2006). Using purified recombinant L protein and in vitro-synthesized short RNA, it was demonstrated that 2'-O methylation of VSV precedes and facilitates subsequent G-N-7 methylation, and two methylase activities require different RNA sequence and length in methylation (Rahmeh et al., 2009). Therefore, VSV cap methylation is mechanistically different from all other known mRNA cap methylation reactions.

Although VSV mRNA MTase has been genetically and biochemically characterized, the mechanism by which a single region VI of L protein catalyzes two methylations is not fully understood. To acquire methylation, the MTase usually directly or indirectly contacts RNA

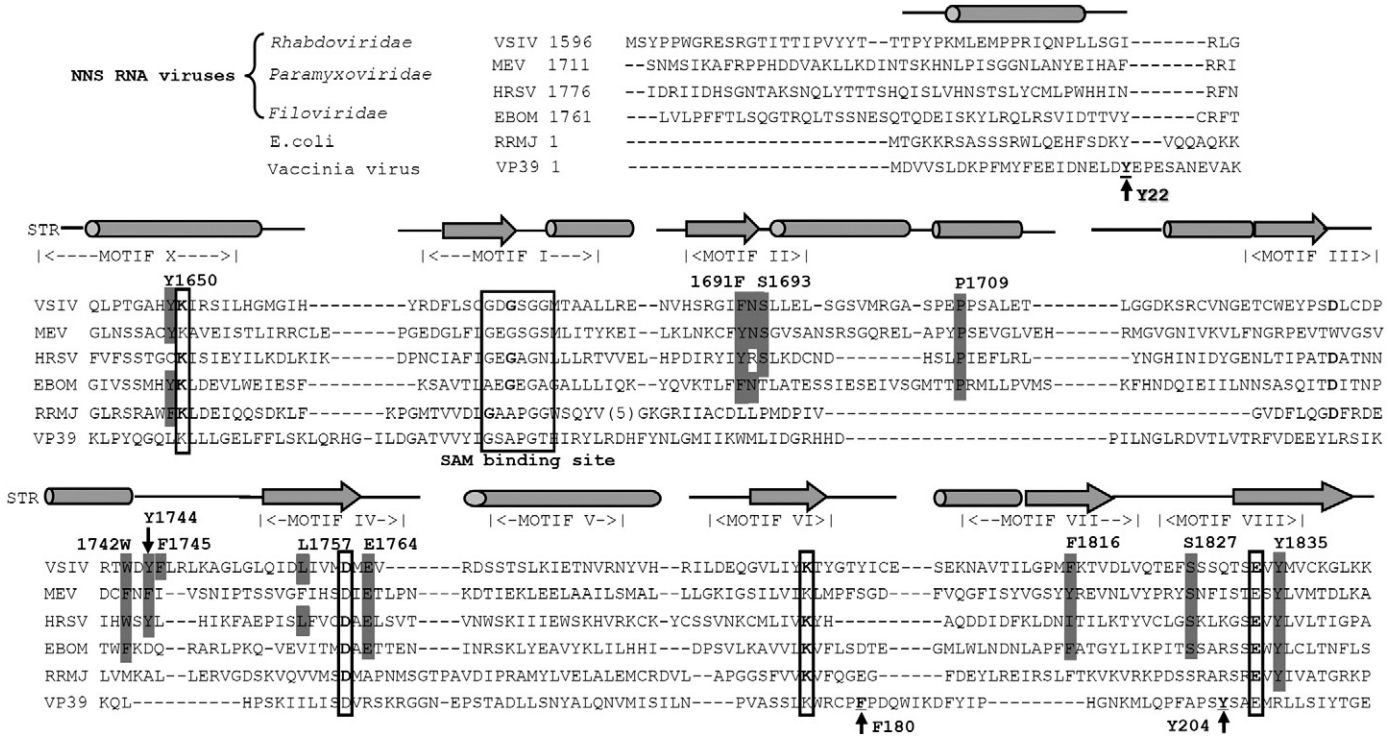

Fig. 1. Structure-based amino acid sequence alignments of conserved domain VI of representative NNS RNA virus L proteins with known 2'-O methyltransferase, the *E. coli* RrmJ and vaccinia virus VP39. The conserved motifs (X and I to VIII) correspond to the SAM-dependent MTase superfamily (Schluckebier et al., 1995). Residues modified in the present study are shaded. MTase catalytic and SAM binding are shown by boxes. Predicted alpha-helical regions are shown by the cylinders and the ß-sheet regions by the arrows. STR, structure of RrmJ and predicted structure for the NNS RNA viruses; EBOM, Ebola virus; VSIV, VSV Indiana type; HRSV, human respiratory syncytial virus; RRMJ, *E. coli* heat shock 2'-O MTase; VP39, vaccinia virus 2'-O MTase VP39.

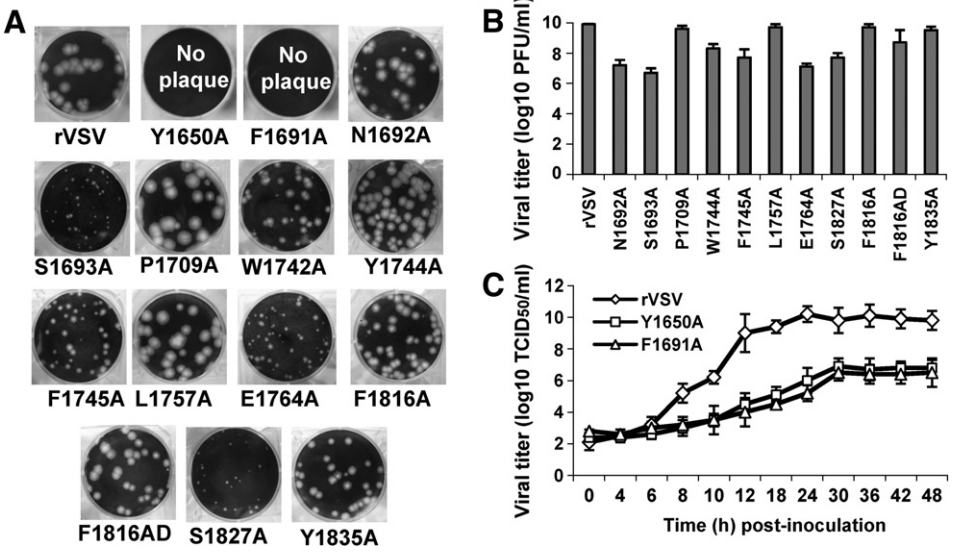

Fig. 2. Recovery of recombinant VSV with mutations in the *L* gene. (A) The plaque morphology of each of the recombinant viruses is shown compared to rVSV. Plaques were developed after 24 h of incubation. Recombinants Y1650A and F1691A did not form plaques. (B) Viral titer of recombinant VSV in BSRT7 cells. BSRT7 cells were inoculated with each of the indicated viruses at an MOI of 3, and the viral yield was determined at 24 hpi by plaque assay. (C) Single-step growth curve of recombinant VSV in BHK-21 cells. Confluent BSRT7 cells were infected with individual viruses at a $TCID_{50}$ of 20. After 1-h incubation, the inoculum was removed, the cells were washed with DMEM, and fresh medium (containing 2% fetal bovine serum) was added, followed by incubation at 37 °C. Samples of supernatant were harvested at the indicated intervals over a 48-h time period, and the virus titer was determined by $TCID_{50}$. Titers are expressed as the mean ± the standard deviation of three independent single-step growth experiments.

substrate (Lockless et al., 1998; Hu et al., 1999; Quiocho et al., 2000; Shuman, 2001; Li et al., 2004; Cowling, 2010). However, this putative substrate binding site has not been suggested for any of the NNS RNA viruses. In this study, we performed further sequence alignment and structure prediction of VSV MTase that suggested several aromatic residues in region VI of VSV L protein as the putative RNA binding site. Subsequently, we performed a systematic mutagenesis analysis of this putative substrate binding site and determined its role in mRNA cap methylation. We demonstrated that the mutation to the aromatic residue abolished both G-N-7 and 2'-O methylations. Although RNA binding has not been directly measured in this study, combined with the structural prediction, our results suggest that these aromatic residues may participate in RNA recognition.

Results

Prediction of putative substrate binding site in VSV MTases and mutagenesis strategy

Based on sequence alignment and structure modeling, domain VI of the L protein in NNS RNA viruses shares homology with known 2'-O-MTases such as vaccinia virus VP39 and *Escherichia coli*. RRMJ (Bujnicki and Rychlewski, 2002; Ferron et al., 2002). To acquire methylation, the RNA substrate must come in contact with the MTase. RNA cap recognition often requires stacking between the base of the cap and aromatic rings from a protein (Lockless et al., 1998; Hu et al., 1999; Quiocho et al., 2000; Egloff et al., 2002; Decroly et al., 2008). The crystal structure of a complex comprising vaccinia VP39, the methylation inhibitor SAH, and an mRNA analog 5' 7^{m}Gppp-capped single-stranded RNA hexamer has been solved (Hodel et al., 1996; Hodel et al., 1998; Hu et al., 1999). It was found that the recognition of a methylated base is achieved by stacking between two aromatic residues (Y22 and F180), and the methyl group is in contact with residue Y204. In addition, the carboxyl groups of residues D182 and E233 form hydrogen bonds to the NH and NH2 of the guanosine in VP39.

In an attempt to identify the putative cap recognition site in VSV MTases, our strategy was to select conserved residues in region VI of L proteins of NNS RNA viruses that are physicochemically similar to those involved in substrate recognition in VP39. Sequence alignment showed that there are a number of aromatic residues that are highly conserved in the MTase domain of L proteins (Fig. 1). Aromatic residues at positions 1650 (Y), 1691(F or Y), and 1835 (Y) are highly conserved in L proteins of NNS RNA viruses although there are some exceptions. For example, these aromatic residues are not conserved in nuclear BDV; 1691(F or Y), and 1835 (Y) are absent in plant rhabdovirus; and 1650 (Y) is not conserved in HRSV (Fig. 1). Aromatic residues at positions 1742 (W), 1744 (Y), 1745 (F) and 1816 (F) are conserved in the L proteins of *Rhabdoviridae* and some *Paramyxoviridae* and *Filoviridae*. Therefore, these aromatic residues were selected as putative equivalents of Y22, F180, and Y204 in VP39. Unfortunately, there is no amino acid precisely aligned with D182 and E233 in VP39. With the exception of two acidic amino acids in the catalytic site (K1651-D1762-K1795-E1833), position E1764 is also conserved in all L proteins. In addition, D1735 is highly conserved although it is W in L protein of some viruses, such as measles virus (Fig. 1). Actually, residue D1735 is a part of the SAM binding motif (GxGxG……D). Previously, we have shown that an alanine substitution for D1735 diminished both G-N-7 and 2'-O methylations to 35% of the level of rVSV (Li et al., 2006). Thus, we targeted E1764 as a candidate for the role of VP39 residues D182 and E233. Finally, other highly conserved amino acid residues (N1692, S1693, P1709, L1757 and S1827) within domain VI of L proteins were also selected for mutagenesis. Previously, a serine residue has been shown to be involved in RNA-protein interaction of *E. coli*. 2'-O MTase, RRMJ (Hager et al., 2004). Therefore, we selected the most conserved serine residues (S1693 and S1827) for mutagenesis.

Recovery of recombinant viruses with L gene mutations

To test our prediction, we first performed alanine scanning mutagenesis in the putative RNA substrate binding site. All of the above amino acid residues were mutated into alanine individually in the *L* gene of an infectious clone of VSV. Recombinant VSV carrying these mutations were recovered from cDNA clone as described in Materials and methods. As shown in Fig. 2A, each of the *L* gene mutations yielded viable recombinant virus. However, most viruses showed defects in viral growth as judged by their plaque morphology.

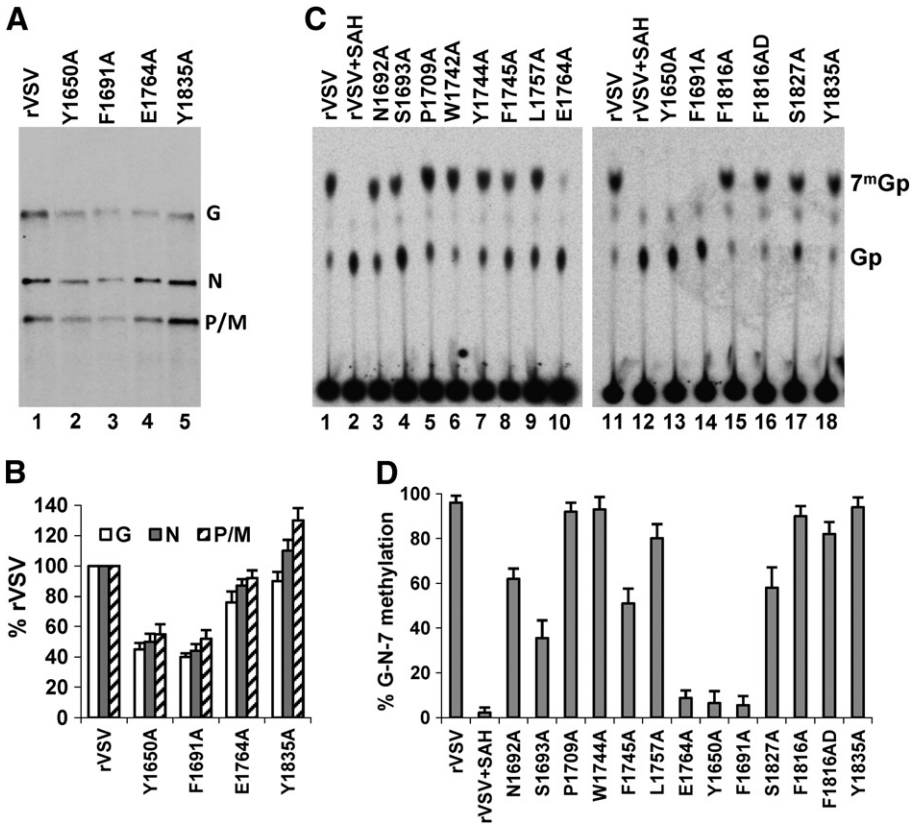

Fig. 3. Effect of *L* gene mutations on mRNA G-N-7methylation in vitro. (A) Synthesis of viral mRNA in vitro. Transcription reactions were performed in vitro in the presence of [α-^{32}P] GTP, the RNA was purified and analyzed by electrophoresis on acid-agarose gels. The products were detected by phosphorimager. The identity of VSV mRNA (G, N, and P/M) is shown on the right. (B) Quantitative analysis of synthesized mRNA for each recombinant virus. Three independent experiments were shown. For each mRNA the mean ± the standard deviation was expressed as a percentage of that observed for rVSV. (C) Analysis of G-N-7 methylation by TLC. Viral mRNA was synthesized in vitro in the presence of 15 μCi [α^{32}P] GTP. The RNA was purified, digested with 2 units of TAP, and subjected to TLC on PEI-F cellulose sheets in 1.2 M $LiCl_2$ solution. The plates were dried, and the spots were visualized using a phosphorimager. The migration of the markers 7^{m}Gp and Gp is indicated. (D) Quantitative analysis of G-N-7 methylation from three independent experiments. For each virus, the released 7^{m}Gp was expressed as a percentage of the total released cap structure (7^{m}Gp and Gp). Data are shown as the mean ± the standard deviation.

After 24 h of incubation, rVSV formed plaques that were 4.3 ± 0.8 mm in diameter. However, alterations to amino acid residues S1693, W1742, F1745, E1764, S1827, and Y1835 resulted in formation of significantly smaller plaques. After 48 h of incubation, the average plaque diameter was 0.6 ± 0.2 mm for S1693A, 2.3 ± 0.4 mm for W1742A, 1.9 ± 0.4 mm for F1745A, 1.3 ± 0.4 mm for E1764A, and 0.9 ± 0.2 mm for S1827A, 2.8 ± 0.4 mm for Y1835A (Fig. 2A). Most interestingly, two recombinant viruses F1691A and Y1650A did not form plaques in either Vero or BSRT7 cells, although they were able to produce significant cytopathogenic effect (CPE) in both cell lines. This suggests that these two recombinants had a defect in cell-to-cell spread. Therefore, the viral titer for these two viruses was determined by $TCID_{50}$ method in BSRT7 cells. The entire *L* gene of each virus was amplified by RT-PCR, sequenced, and the presence of the desired mutation was confirmed in all of the viruses. With the exception of the F1816A-mutated virus, no additional mutations were identified. Virus F1816A contained one additional nucleotide change G10177T which resulted in coding change M1815I. Thus, this virus was named F1816AD. Subsequently, we isolated a fresh F1816A from an independent transfection, and sequence confirmed that no additional changes were present within the *L* gene.

To examine the effect of these mutations on viral growth, we determined the virus yield in infected cells. Briefly, BSRT7 cells were infected with each virus at a MOI of 3 and the viral titer was determined at 24 h after inoculation. Recombinants E1764A, N1692A, S1693A and S1827A had a 3 logarithmic growth defect compared with rVSV (Fig. 2B). Recombinants W1744A and F1745A had a 2 logarithmic growth defect (Fig. 2B). Since recombinant F1691A and Y1650A were not able to form plaques, we monitored the kinetics of release of infectious virus by single-step growth assay in BSRT7 cells using $TCID_{50}$ assay by Reed–Muench method (Reed and Muench, 1938). Briefly, BSRT7 cells were infected with 20 $TCID_{50}$ of each of the indicated recombinants and viral replication was determined at time points from 0 to 48 h postinfection. As shown in Fig. 2C, both F1691A and Y1650A had significant defects in viral replication as compared to that of rVSV. Wild type rVSV reached peak titer ($10^{9.8}$ $TCID_{50}$/ml) at 12 h post-infection. However, both Y1650A and F1691A reached peak titer ($10^{6.4}$ $TCID_{50}$/ml) at 30 h post-infection. Taken together, these results demonstrate that amino acid substitutions in the putative RNA binding site significantly diminished viral replication.

Identification of amino acids in the putative RNA substrate binding site that are essential for G-N-7 methylation

To examine the effect of amino acid substitutions in the putative RNA binding site on mRNA cap methylation, in vitro transcription reactions were performed as described previously (Li et al., 2005). Briefly, 20 μg of virus was activated with detergent and incubated with nucleoside triphosphates supplemented with [α-^{32}P]GTP as described in Materials and methods. Total RNA was extracted, purified, and analyzed by acid-agarose gel electrophoresis as described previously (Li et al., 2005). All of the recombinant viruses were able to synthesize similar amounts of mRNA except for F1691A and Y1650A. These two recombinants synthesized approximately 50%

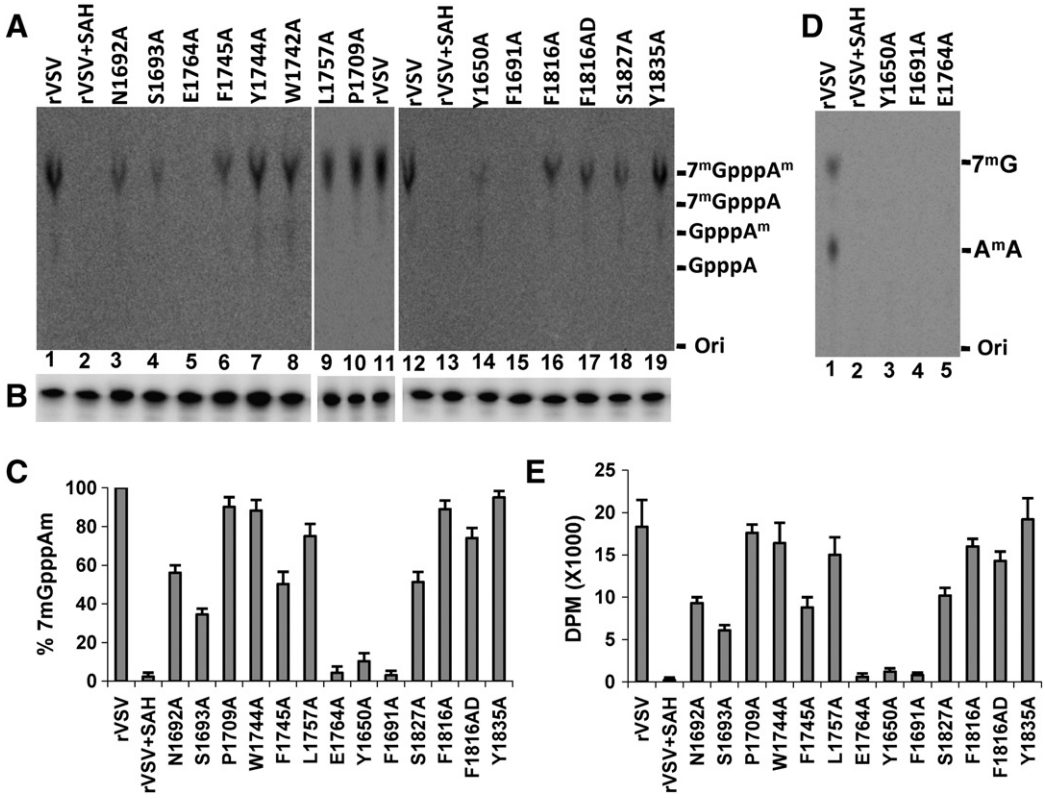

Fig. 4. Effect of *L* gene mutations on mRNA G-N-7 and 2'-O methylation in vitro. (A) Analysis of mRNA cap methylation by nuclease P1 digestion. Viral mRNA was synthesized in the presence of [^{3}H]SAM, the RNA were purified and digested with 5 unit of nuclease P1, and the products were developed on PEI-F cellulose sheets. The plates were dried, and the spots were visualized by phosphorimage analysis. (B) Primer extension of viral mRNA. RNA from panel A was examined by primer extension using a primer designed to anneal to the N mRNA. Products were developed by electrophoresis on denaturing 6% polyacrylamide gels. (C) Quantitative analysis of G-N-7 and 2'-O methylation from three independent experiments. For each virus, methylation was expressed as a percentage of the released ^{7m}GpppA^m compared to that of rVSV. Data were shown as the mean ± the standard deviation. (D) Analysis of mRNA cap methylation by RNase T2 and TAP. Purified RNAs were digested with TAP and RNase T_2 prior to TLC analysis. The migration of the ^{7m}Gp marker is shown, and the presumed pA^{m}pAp spot is identified. (E) Measurement of mRNA cap methylation by [^{3}H]SAM incorporation using scintillation counting. Data were calculated from three independent experiments.

of the level of the rVSV mRNA (Fig. 3A and B). To compensate for these defects in mRNA synthesis, the amount of these viruses used in the in vitro transcription reactions was increased to 40 μg.

To analyze the G-N-7 methylation, 8.8 μl of each in vitro-synthesized mRNA was treated by TAP. TAP specifically cleaves the pyrophosphate bond of the GpppN cap to yield Gp or, if the cap structure is methylated, ^{7m}Gp. These products are resolved by TLC on polyethyleneimine (PEI) cellulose F sheets. For rVSV, when transcription reactions were performed in the presence of 1 mM SAM, a fully G-N-7 methylated cap (^{7m}Gp) was detected after TAP digestion (Fig. 3C, lane 1). This radioactive spot co-migrated with the marker ^{7m}Gp as visualized by UV shadowing. However, an unmethylated cap (Gp) was detected when the transcription reaction was performed in the presence of 100 μM SAH (Fig. 3C, lane 2). Quantitative analysis of three independent experiments showed that the total of 14 mutants can be classified into three different groups (Fig. 3C and D). Viruses in the first group abolished G-N-7 methylation. These viruses included Y1650A, F1691A, and E1764A, which yielded 6.5%, 5.5%, and 8.8% of G-N-7 methylated cap, respectively. Viruses that had a moderate defect in G-N-7 methylation were classified into group 2. These viruses included N1692A, S1693A, F1745A, and S1827A, which yielded 30-60% of G-N-7 methylated cap. Viruses that did not have a significant defect in G-N-7 methylation were classified into group 3. This group includes P1709A, W1744A, L1757A, F1816A, F1816AD, and Y1835A. These data clearly demonstrate that alterations to two aromatic amino acid residues (Y1650A and F1691A) and one acidic residue (E1764A) abolish G-N-7 methylation.

Identification of amino acids in the putative RNA substrate binding site that are essential for both G-N-7 and 2'-O methylation

To examine the effect of these mutations on both G-N-7 and 2'-O methylations, in vitro transcription reactions were performed in the presence of [^{3}H]SAM. Total RNAs were extracted, purified, and subjected to nuclease P1 digestion followed by TLC on PEI cellulose F sheets. Nuclease P1 cleaves the bond between the 3′-hydroxyl and 5′-phosphoryl group of adjacent nucleosides. Theoretically, digestion of VSV mRNAs by P1 should yield ^{7m}GpppA^m (double methylated), GpppA^m (only 2'-O methylated), ^{7m}GpppA (only G-N-7 methylated), or GpppA (unmethylated), depending on the extent of cap methylation. The standard markers for these products were visualized by UV shadowing. For rVSV, when transcription reactions were performed in the presence of 50 μM of [^{3}H]-SAM, a doubly methylated cap (^{7m}GpppA^m) was detected after P1 digestion (Fig. 4A, lane 1). However, no detectable products were observed when 1 mM of SAH was included in the reaction, confirming that both G-N-7 and 2'-O methylations were completely inhibited (Fig. 4A, lane 2). Phenotypes of a total of 14 mutants are shown in Fig. 4A.

Quantitative analysis of three independent experiments showed that these mutants fall into three categories (Fig. 4C). Recombinants Y1650A, F1691A, and E1764A reduced both G-N-7 and 2'-O methylations to an undetectable level (Fig. 4A and C). Recombinants N1692A, S1693A, F1745A, and S1827A were able to synthesize doubly methylated cap. However, the abundance of a fully methylated cap was diminished 30-60%. Viral mutants defective in G-N-7 methylation

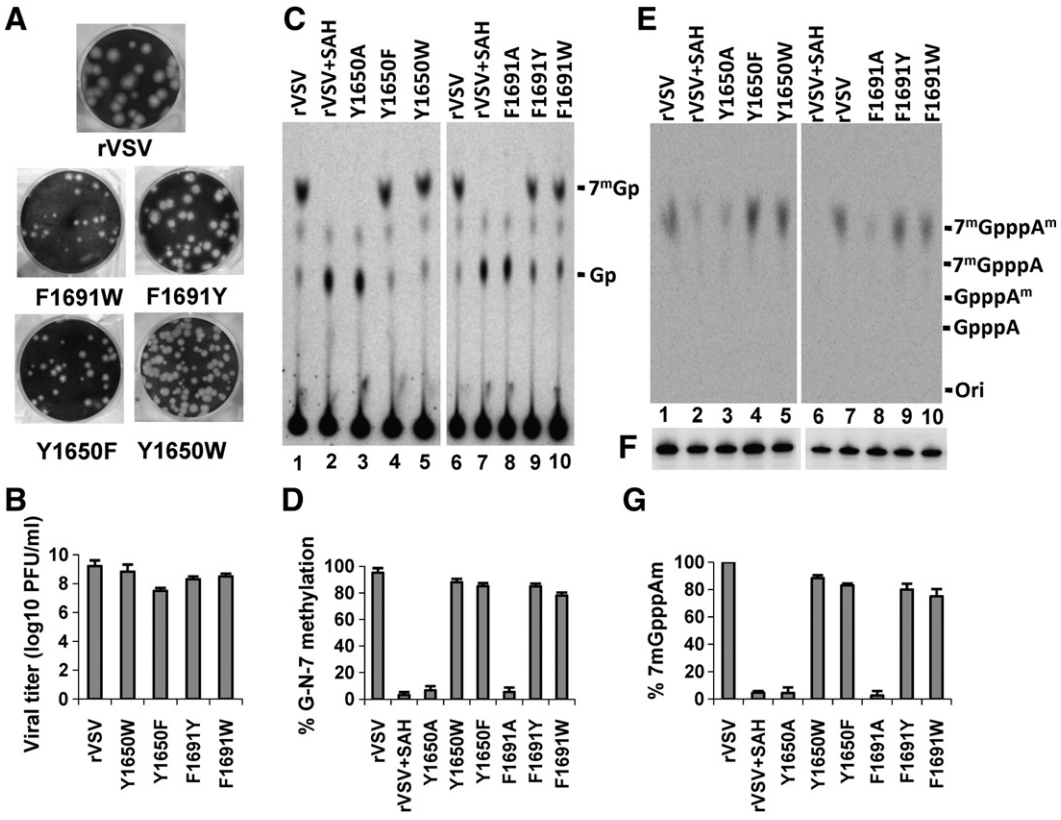

Fig. 5. The role of Y1650 and F1691 in mRNA cap methylation. (A) The plaque morphology of each of the recombinant viruses carrying mutation in Y1650 and F1691. Plaques were developed after 24 h of incubation. (B) Viral titer of recombinant VSV in BSRT7 cells. BSRT7 cells were infected by indicated viruses at an MOI of 3, and the viral yield was determined at 24 hpi. (C) Analysis of G-N-7 methylation by TAP digestion. Purified RNAs were digested by TAP, and the products were developed on PEI-F cellulose sheets. The markers 7^{m}Gp and Gp were shown. (D) Quantitative analysis of G-N-7 methylation from three independent experiments. (E) Analysis of G-N-7 and 2'-O methylation by nuclease P1 digestion. Viral mRNA was synthesized in the presence of [^{3}H]SAM, purified RNA were digested with 5 unit of nuclease P1, and the products were developed on PEI-F cellulose sheets. (F) RNA from panel E was examined by primer extension using a primer designed to anneal to the N mRNA. (G) Quantitative analysis of G-N-7 and 2'-O methylations from three independent experiments.

were also equally defective in 2'-O methylation. Recombinants P1709A, W1744A, L1757A, F1816A, and F1816AD, and Y1835A yielded similar amounts of doubly methylated cap compared to that of rVSV, confirming that they did not affect either G-N-7 or 2'-O methylation (Fig. 4A and C). Interestingly, none of the viral mutants was defective only either in G-N-7 or 2'-O methylation. To further confirm these results, we performed additional cap hydrolysis. The RNA samples from rVSV, Y1650A, F1691A and E1764A were digested by RNase T2 and TAP. RNase T2 is an endoribonuclease that cleaves the phosphodiester bonds on the 3' side of A residues. Digestion of the VSV mRNA cap structure with RNase T2 should yield 7^{m}GpppA^{m}A if the cap structure was doubly methylated. Further digestion of this product by TAP would yield 7^{m}G and A^{m}A. As shown in Fig. 4D, double digestion of RNA synthesized from rVSV yielded two radioactive spots. The first spot comigrated with the 7^{m}Gp marker, representing G-N-7 methylation. Presumably, the second spot was A^{m}A, representing 2'-O methylation. The identity of these spots was also consistent with our previous publications (Li et al., 2005, 2006). However, these two spots were undetectable in RNA synthesized from rVSV in the presence of SAH, Y1650A, F1691A, and E1764A (Fig. 4D, lanes 2–5), confirming that both G-N-7 and 2'-O methylations were abolished. To ensure there is an equivalent amount of RNA synthesized from each mutant, a primer extension assay was performed to detect the first 130 nt of N mRNA. As shown in Fig. 4B, the amount of RNA used for cap hydrolysis is indistinguishable for each mutant. Therefore, these results further confirmed that Y1650A, F1691A, and E1764A lack both G-N-7 and 2'-O methylations.

To further confirm the extent of cap methylation, the amount of [^{3}H]-SAM incorporated into the viral mRNA was measured by scintillation counting and the dpm normalized to the amount of RNA synthesized. As shown in Fig. 4E, the amount of [^{3}H] for recombinants Y1650A, F1691A and E1764A was about 5-10% that of rVSV. The amount of [^{3}H]-SAM incorporation for recombinants N1692A, S1693A, F1745A, and S1827A was about 30–50% of that of rVSV. Recombinant P1709A, W1744A, L1757A, F1816A, and F1816AD, and Y1835A viruses showed comparable levels of [^{3}H]-SAM incorporation to that of rVSV. Again, these results are consistent with cap hydrolysis by nuclease P1 digestion. Taken together, these experiments demonstrate that alanine substitutions for two aromatic residues (Y1650A and F1691A) and an acidic residue (E1764A) in VSV MTase abolish both G-N-7 and 2'-O methylation.

Cap methylation requires maintenance of two aromatic residues

It has been demonstrated that RNA cap recognition typically requires stacking between the base of the cap and aromatic rings from a protein (Lockless et al., 1998; Hodel et al., 1998; Hu et al., 1999; Quiocho et al., 2000; Egloff et al., 2002; Decroly et al., 2008). If aromatic residues are, indeed, involved in RNA cap recognition, maintenance of the aromatic ring may be essential for mRNA cap methylation. To further demonstrate the role of aromatic residues F1691 and Y1650 in VSV mRNA cap methylation, each of these two aromatic residues were changed to two other possible aromatic residues (Y, W or F) in the VSV infectious clone. A total of four possible mutants (F1691Y, F1691W, Y1650F, and Y1650W) were generated. As shown in Fig. 5A, each of these mutations yielded viable recombinant virus. Interestingly, changing from one aromatic residue to another aromatic residue did not significantly affect the size of viral plaques.

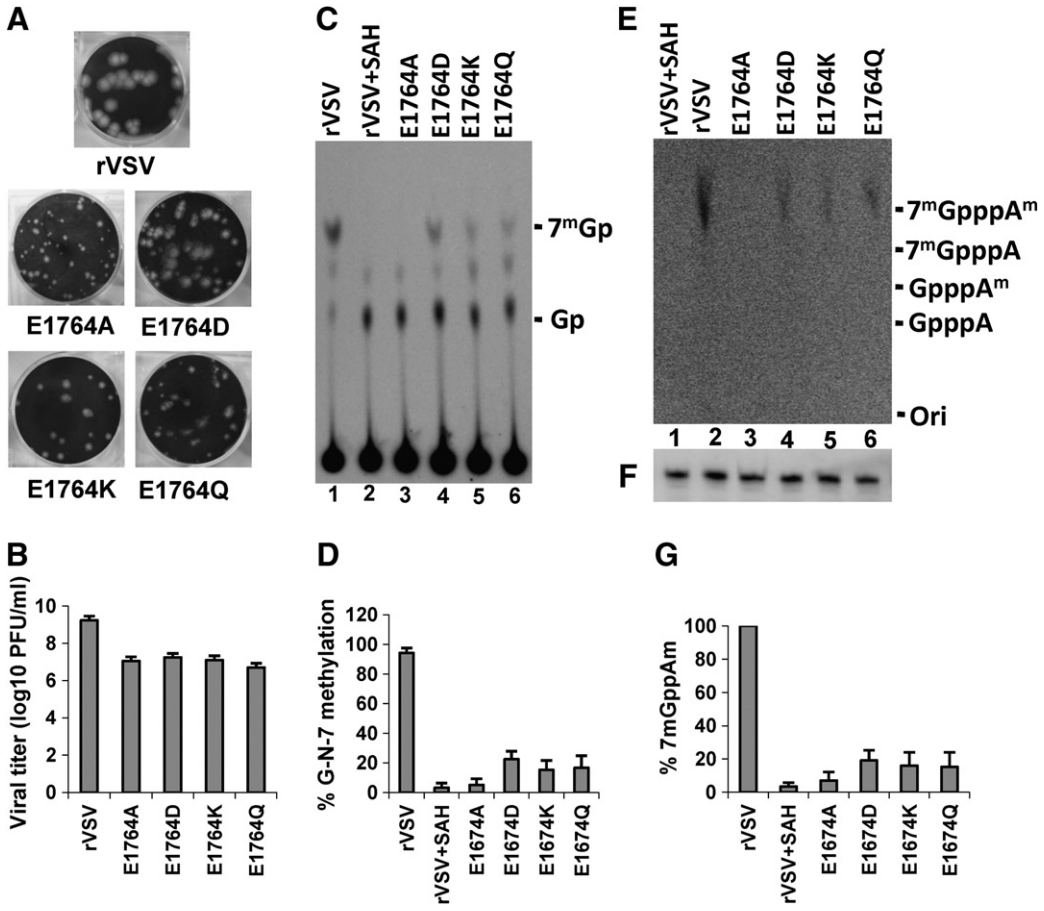

Fig. 6. The role of E1764 in mRNA cap methylation. (A) The plaque morphology of each of the recombinant viruses carrying a mutation for E1764. Plaques were developed after 24 h of incubation. (B) Viral titer of recombinant VSV in BSRT7 cells. BSRT7 cells were infected by indicated viruses at an MOI of 3, and the viral yield was determined at 24 hpi. (C) Analysis of G-N-7 methylation by TAP digestion. Purified RNAs were digested by TAP, and the products were developed on PEI-F cellulose sheets. (D) Quantitative analysis of G-N-7 methylation from three independent experiments. (E) Analysis of G-N-7 and 2'-O methylation by nuclease P1 digestion. (F) RNA from panel E was examined by primer extension using a primer designed to anneal to the N mRNA. (G) Quantitative analysis of G-N-7 and 2'-O methylations from three independent experiments.

All these viruses replicated to high titer in BSRT7 cells, indistinguishable from that of rVSV (Fig. 5B). In sharp contrast, alanine substitutions for these aromatic residues resulted in recombinant viruses that did not form plaques (Fig. 2A) and significantly diminished viral replication (Fig. 2C). These data suggest that maintenance of an aromatic residue at positions 1691 and 1650 is essential for viral replication.

To examine G-N-7 methylation, in vitro transcription reactions were performed in the presence of [α-32P]GTP. The RNA was purified as described, the cap structure was hydrolyzed with TAP, and the products were analyzed by TLC on PEI-F cellulose sheets. TAP digestion demonstrated that F1691Y and F1691W mutants exhibited 85% and 82% of the rVSV G-N-7 methylation, respectively (Fig. 5C). Y1650F and Y1650W mutants showed 88% and 90% of the rVSV G-N-7 methylation, respectively (Fig. 5C and D). Thus, changing from one aromatic residue to another aromatic residue does not significantly affect G-N-7 methylation.

To examine 2'-O methylation, the in vitro transcription reaction was performed in the presence of [3H]-SAM. The RNAs were purified and subjected to nuclease P1 digestion. P1 digestion showed that all of these mutants were able to synthesize doubly methylated caps (Fig. 5E). Quantitative analysis showed that Y1650F, Y1650W, F1691Y, and F1691W yielded 90%±2%, 90%±3%, 88%±4%, and 80%±5% of $7^{m}GpppA^{m}$, respectively (Fig. 5G). Primer extension showed that there were equivalent amounts RNA synthesized from each mutant (Fig. 5F). Thus, these data demonstrate that other aromatic residues can substitute for Y1650 and F1691 in the VSV MTase. These results suggest that VSV mRNA cap methylation may require the stacking interaction between the base of the cap and an aromatic residue at position 1650 and 1691.

The role of E1764 in VSV mRNA cap methylation

To further characterize the role of E1764 in VSV mRNA cap methylation, we mutated this residue to D (maintenance of charge), Q (maintenance of size) or K (changing charge). Using reverse genetics, recombinant viruses carrying these mutations were successfully recovered. As shown in Fig. 6A, the plaque sizes of E1764D, E1764Q and E1764K-mutated viruses were significantly diminished as compared to that of rVSV. These recombinants have a moderate defect (2-3 log viral yields) in replication in BSRT7 cells (Fig. 6B).

The in vitro transcription reaction was performed using purified viruses and mRNA cap methylation was analyzed as described above. As shown in Fig. 6C, these recombinant viruses are defective in G-N-7 methylation compared to rVSV. Quantitative analysis showed that E1764D, E1764Q and E1764K yielded 22%±5%, 17%±8%, and 15%±6% of $7^{m}Gp$, respectively (Fig. 6D). Nuclease P1 digestion showed that E1764D, E1764Q and E1764K had a significant reduction in both G-N-7 and 2'-O methylation (Fig. 6E), yielding 19% ± 6%, 15%±9%, and 16%±8% of $7^{m}GpppA^{m}$, respectively (Fig. 6G). Equivalent amounts of RNA were synthesized from each mutant as confirmed by primer extension (Fig. 6F). Therefore, changing of residue E at position 1764 to any other amino acids, even the very conservative change to D,

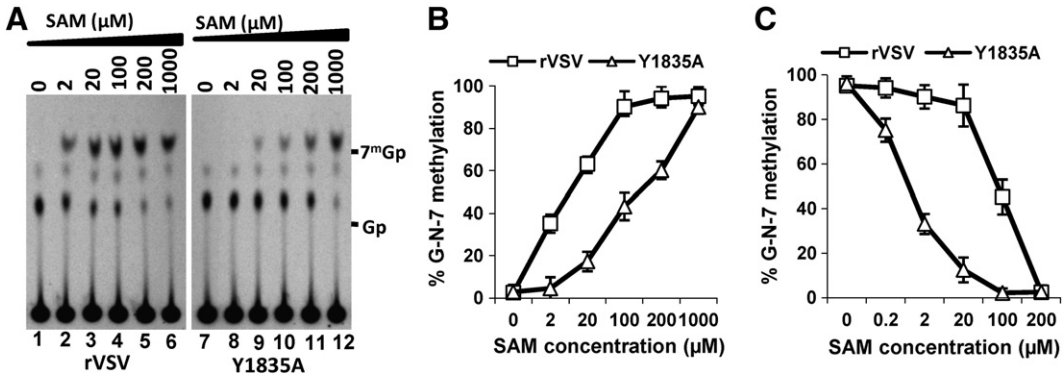

Fig. 7. Effect of SAM and SAH concentration on G-N-7 methylation of rVSV and Y1835A. (A) Viral mRNA was synthesized in vitro in the presence of different concentration of SAM and 15 mCi of [α-^{32}P]GTP without a cell lysate. Purified RNA was digested with 2 units of TAP, and the products were analyzed by TLC on PEI F cellulose sheets. The migration of the markers 7^{m}Gp and Gp is indicated. (B) Recombinant Y1835A requires a higher concentration of SAM for G-N-7 methylation. Quantitative analysis was performed on three independent experiments. For each virus, the released 7^{m}Gp (mean ± standard the standard deviation) was expressed as a percentage of the total released cap structure. (C) G-N-7 methylation of Y1835A is more sensitive to SAH inhibition. Viral mRNA was synthesized in vitro in the presence of 200 μM of SAM without a cell lysate, 15 mCi of [α-^{32}P]GTP, and different concentrations of SAH. Quantitative analysis was performed on three independent experiments.

significantly diminished both G-N-7 and 2'-O methylation. These data suggest that E1764 is critical for both G-N-7 and 2'-O methylation.

Y1835A requires a higher SAM concentration and it is more sensitive to MTase inhibitor

There are a total of 7 aromatic residues that were selected for mutagenesis. Mutants Y1650A and F1691A abolished G-N-7 and 2'-O methylation. F1745A had a moderate reduction in methylation. Other aromatic residues (W1742, Y1744, F1816 and Y1835) did not have a significant impact on mRNA cap methylation. To further characterize the role of these amino acids, we monitored the effect of SAM and SAH concentration on mRNA cap methylation of these mutants. Briefly, an increasing amount of either SAM or SAH was added to the in vitro transcription reaction in the presence of [α-^{32}P]GTP, RNAs were purified and treated with TAP. For rVSV, a full G-N-7 methylation was achieved when the reaction was performed in the presence of 100 μM of SAM (Fig. 7A and B). In contrast, Y1835A requires a much higher SAM concentration (1 mM) to achieve full G-N-7 methylation (Fig. 7A and B). For rVSV, G-N-7 methylation was completely inhibited when 200 μM of SAH was added to the reaction (Fig. 7C). However, Y1835A was much more sensitive to SAH inhibition and G-N-7 methylation was almost completely inhibited by the addition of 20 μM of SAH (Fig. 7C). Thus, these experiments show that Y1835A requires higher SAM concentration for methylation and it is more sensitive to an MTase inhibitor. In contrast, alterations to other three aromatic residues (W1742, Y1744 and F1816) resulted in viruses with properties similar to rVSV (data not shown). These results suggest that an alanine substitution for Y1835 alters the affinity of SAM and SAH in mRNA cap methylation.

Discussion

Prior to this study, the putative RNA substrate recognition site had not been suggested for any MTase in the L protein of NNS RNA viruses. Using the prototype rhabdovirus VSV as a model, we performed a systematic mutagenesis analysis of a putative substrate binding site in the MTase region of L polymerase and determined the effect of these changes on VSV mRNA cap methylation. We found that individual amino acid substitutions to two aromatic residues (Y1650 and F1691) and one acidic amino acid residue (E1764) abolished both G-N-7 and 2'-O MTases. Substitution for F1745 resulted in a moderate defect in both methylations. Mutation of Y1835 resulted in recombinant virus that was more sensitive to SAM and SAH concentration. We further demonstrated that MTase-defective viruses also significantly diminished replication in cell culture. These findings suggest that amino acid residues in VSV methylase are essential for both G-N-7 and 2'-O MTases and may function as a putative RNA recognition site.

Identification of amino acids residues essential for mRNA cap recognition

The structure of several cellular and viral mRNA 2'-O MTases has been determined (Hodel et al., 1996; Hager et al., 2002; Egloff et al., 2002; Zhou et al., 2007). To achieve 2'-O methylation, RNA substrate contacts with the cap recognition site requires stacking between the base of the cap and aromatic rings from a MTase (Bugl et al., 2000; Lockless et al., 1998; Hu et al., 1999; Quiocho et al., 2000; Egloff et al., 2002; Decroly et al., 2008). Vaccinia VP39 is one of the best characterized 2'-O MTases. In VP39, it was found that the recognition of a methylated base is achieved by stacking between two aromatic residues (Y22 and F180) (Hodel et al., 1996; Hu et al., 1999). Based on structure modeling and mutagenesis analysis, it was shown that residue F24 in West Nile virus (WNV) methylase (NS5) (Dong et al., 2007) and Y29 and F173 in feline coronavirus 2'-O MTase (nsp16) (Decroly et al., 2008) may play an equivalent role to residue Y22 in VP39. The cellular cap binding protein eIF4E recognizes the cap by stacking between W56 and W102 (Marcotrigiano et al., 1997). In all known cases, aromatic residues are involved in cap binding and substrate recognition.

Sequence alignment and structure prediction suggest that domain VI of VSV L protein shares homology with known 2'-O MTases. We are particularly interested in the highly conserved aromatic amino acids since they may be involved in cap recognition. Among 7 aromatic residues we selected, Y1650 and F1691 were the most critical amino acids essential for mRNA cap methylation. Specifically, alanine substitutions for Y1650 and F1691 abolished both G-N-7 and 2'-O methylation (Fig. 3C and D). However, replacement of one aromatic residue with another aromatic residue (Y1650F, Y1650W, F1691Y, and F1691W) did not significantly affect the methyltransferase activities (Fig. 5C and E), suggesting that maintenance of the aromatic residue is required for RNA substrate recognition and methylation. Similar to other known 2'-O MTases, these two residues may have a stacking interaction with the mRNA cap that lead to correct positioning of capped RNA into the catalytic site. Based on the predicted structural model for the VSV MTase (amino acid residues from 1644 to 1842 in the L protein) (Galloway et al., 2008), the residues Y1650 and F1691 are located far from each other with a distance of 17.3 Å between their alpha carbon atoms. Y1650 is located in the middle of the first helix, and the F1691 is at the very C-terminal of the second helix (Fig. 8A). Perhaps, a stacking interaction with one aromatic residue causes a conformational and structural change in the VSV methylase, which results in the interaction with another aromatic

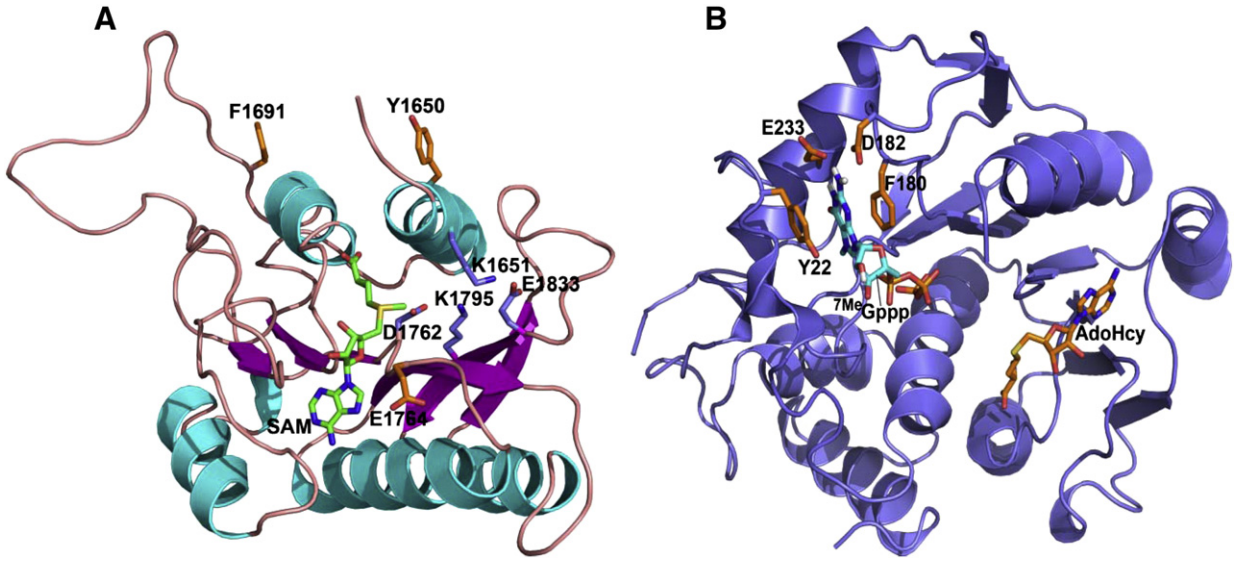

Fig. 8. Critical amino acids in the predicted structure of VSV MTase. (A) The model was generated based on the previous predicted structure of VSV MTase (amino acid residue from 1644 to 1842 in L protein) (Galloway et al., 2008) using PyMOL software. Alpha helices are shown in blue and beta strands are shown in pink. SAM and the side chains of critical residues are shown in sticks, and the oxygen atoms and nitrogen atoms are shown in red and blue, respectively. For SAM molecule, the carbon atoms are green. For the three important amino acids (Y1650, F1691 and E1764) identified in this study, their side-chain carbon atoms are highlighted in orange. For the predicted catalytic residues (K1651, D1762, K1795 and E1833), the carbon atoms are shown in purple. (B) Cap binding site of vaccinia virus 2'-O MTase, VP39. The model was generated from the crystal structure of VP39 (PDB code: 1AV6) using PyMOL. The side chains of amino acid residues (Y22, F180, E233 and D182) involved in binding of 7^{m}Gp cap are shown as sticks.

residue. An alanine substitution for either Y1650 or F1691 may prevent these stacking interactions, which, in turn, affects mRNA methylation. Interestingly, recombinants Y1650A and F1691A were not able to form plaques in either BSRT7 or Vero cells. During the plaque assay, we found that cells in six-well plates were either completely killed or intact without generating regions of cell destruction. However, they were still able to cause cell lysis and produce CPE in both BSRT7 and Vero cells. It is likely that these viruses were replication competent, but had a defect in cell-to-cell spread. In addition, recombinant Y1650A and F1691A synthesized only 50% of viral mRNAs in vitro compared to rVSV (Fig. 3A and B). Perhaps, alanine substitution to Y1650 and F1691 may have an effect on the overall folding and/or stability of L protein.

We also found that F1745 and Y1835 play a role in mRNA cap methylation. Recombinant F1745A exhibited a significant defect in both G-N-7 and 2'-O methylation (Fig. 3C). Interestingly, recombinant Y1835 requires a higher SAM concentration for methylation and it is more sensitive to SAH inhibition (Fig. 7). This is similar to the phenotype we observed in one of the mutants (G1674A) in the putative SAM binding site (Li et al., 2006). Y1835 is conserved in the L proteins of almost all NNS RNA viruses and is adjacent to catalytic residue E1833. Most likely, substitution for Y1835 altered the affinity to bind the SAM molecule or affected catalysis.

In VP39 structure, D182 and E233 also make contact with guanosine (Hodel et al., 1996). We targeted E1764 as a candidate for the role of D182 and E233 in VP39. Substitution of E1764 to A, D, Q or K abolished both G-N-7 and 2'-O methylations (Fig. 6). The predicted structure of VSV MTase also shows that E1764, the residue adjacent to the catalytic residue D1762, is exposed to the putative SAM binding site. The side chain of E1764 shows close contact to the adenyl group of SAM (3.1 Å) (Fig. 8A). However, these residues are located at different sides of the cavity of the SAM-binding and catalytic sites. Y1650 and F1691 are on one side, whereas E1764 is on the other, and the side chains of these three residues are all exposed outward from the cavity. E1764 is apart from residues Y1650 and F1691 in the alpha-carbon atom distances of 16.8 and 27.0 Å, respectively. Perhaps, E1764 may be critical for catalysis, SAM binding, or the interaction with the RNA chain, instead of mediating contact with mRNA cap. In addition, we also found that other amino acid substitutions such as N1692A, S1693A and S1827A affected mRNA cap methylation (Fig. 3C). Interestingly, S197 in RRMJ has been shown to be involved in RNA-protein interactions (Hager et al., 2004). Further functional and structural studies of the VSV MTase will be necessary to define the exact role of these amino acids in mRNA cap methylation.

Model for mRNA cap recognition in a dual MTase

Our structure prediction and mutagenesis is guided by the homology of VSV MTase with 2'-O MTases. If Y1650 and F1691 are the cap recognition site for VSV 2'-O MTase, why does alteration in these amino acid residues also abolish G-N-7 methylation? Perhaps, the simplest explanation is that the order of VSV mRNA cap methylation is unique in which 2'-O methylation is required for G-N-7 methylation (Li et al., 2006; Rahmeh et al., 2009). Thus, inhibition of 2'-O methylation would likely also prevent the G-N-7 methylation. Another model is that aromatic residue Y1650 and F1691 also make contact with the mRNA cap during G-N-7 methylation. Previously, it was thought that no amino acid residue was in direct contact with the guanine-N-7 nucleophile, the SAM methyl carbon, or the SAH sulfur leaving group (Fabrega et al., 2004). Rather, cap G-N-7 methylation is accomplished by optimally orienting the substrates in proximity to facilitate methyl transfer (Fabrega et al., 2004). However, a recent structural study of vaccinia G-N-7 MTase revealed that aromatic residues (Y555 and F556) play a critical role in G-N-7 methylation (De la Pena et al., 2007; Zheng and Shuman, 2008a,b). These aromatic amino acids stabilize binding to the catalytic site and facilitate the precise positioning of the methyl donor. Therefore, we cannot exclude the possibility that Y1650 and F1691 play a role in stabilizing the binding of VSV MTase to the cap during G-N-7 methylation.

Of course, it would be of great interest to test whether mutations to aromatic residues influence binding of the RNA substrate in vitro. In an attempt to demonstrate the RNA binding activity, we expressed and purified the recombinant L mutant carrying both F1961A and Y1650A, and their RNA binding activities were determined by a gel shift assay. Unfortunately, these amino acid changes did not affect the RNA binding activity in vitro (data not shown). It is likely that there are many RNA binding sites in the 240-kDa L protein and a single point mutation in MTase may not affect the RNA-protein complex.

A single region in the polymerase protein catalyzes dual MTases

In eukaryotic cells, G-N-7 and 2'-O MTases are usually catalyzed by separate proteins and each protein encodes its own SAM binding site (Barbosa and Moss, 1978; Schluckebier et al., 1995; Shuman, 2001). In the case of reovirus, two methylase activities are located in two different domains in a single protein and each domain possesses a SAM binding motif (Reinisch et al., 2000). To date, rhabdovirus VSV and flavivirus WNV are the two best characterized viruses that utilize a single region in the polymerase protein for both G-N-7 and 2'-O methylations. However, the mechanism of VSV mRNA methylation is distinct from that of the WNV system. In VSV, 2'-O methylation precedes and facilitates subsequent G-N-7 methylation (Li et al., 2006; Rahmeh et al., 2009). However, WNV MTases modify the cap structure, first at the G-N-7 position and subsequently at the ribose 2'-O position (Ray et al., 2006; Zhou et al., 2007; Dong et al., 2007). In VSV, G-N-7 and 2'-O MTases require similar conditions for methylation with an optimal pH at 7.0 (Rahmeh et al., 2009). In contrast, G-N-7 and 2'-O MTases of WNV require an optimal pH at 6.5 and 10, respectively (Ray et al., 2006). Both VSV and WNV MTases modify the RNA in a sequence-specific manner, but require different elements in the RNA substrate. VSV G-N-7 and 2'-O MTases require specific gene start sequences with a minimum mRNA length of 10 nucleotides (Wang et al., 2007; Rahmeh et al., 2009). In the WNV model, N-7 cap methylation requires specific nucleotides at the second and third positions and a 5' stem-loop structure within the 74-nucleotide viral RNA; in contrast, 2'-O ribose methylation requires specific nucleotides at the first and second positions, with a minimum 5' viral RNA of 20 nucleotides (Dong et al., 2007).

In this study, we found that there is another striking difference in the cap recognition site between VSV and WNV MTases. In WNV MTase, the cap recognition site is essential for 2'-O, but not G-N-7 methylation (Dong et al., 2008). Consistent with this, GTP and cap analogs specifically inhibited 2'-O, but not G-N-7 methylation (Dong et al., 2008). It was proposed that WNV MTase catalyzes two methylations through a substrate-repositioning mechanism, in which the G-N-7 methylated cap is repositioned to the cap binding site for 2'-O methylation upon binding (Dong et al., 2008). However, it is unlikely that the RNA substrate binding site functions as a switching point for VSV MTase since substitutions to this site abolished both G-N-7 and 2'-O methylations. In agreement with this hypothesis, GTP and cap analogs did not affect VSV mRNA cap methylation in vitro (Li et al., unpublished observation). Previously, we and others have performed extensive mutagenesis analysis in the MTase catalytic and SAM binding sites (Li et al., 2005, 2006, 2007; Grdzelishvili et al., 2005; Galloway and Wertz, 2008). Some of the mutants (G1670A and G1672A) in the SAM binding site were defective in G-N-7, but not 2'-O methylation (Li et al., 2006). Interestingly, none of the mutants were specifically defective in 2'-O, but G-N-7 methylation. Most likely, the cap recognition site in VSV MTase plays an essential role in stacking the cap of the RNA substrate during 2'-O methylation and possibly stabilizes the RNA-MTase complex during G-N-7 methylation. Overall, the mechanism of VSV mRNA cap methylation is significantly different that of WNV, although both of them encode dual MTase activities in a single domain in viral polymerase proteins. Most recently, it was found that capping of flavivirus RNA is catalyzed by conventional RNA guanylyltransferase via a covalent GMP-enzyme intermediate (Issur et al., 2009). However, VSV capping is catalyzed by a novel polyribonucelotidyltransferase (PRNTase) (Ogino and Banerjee, 2007; Li et al., 2008; Ogino et al., 2010; Koonin and Moss, 2010). These studies suggest that VSV and perhaps other NNS RNA viruses have evolved a unique mechanism to add the cap to their mRNA and to methylate the cap structure.

In summary, we examined the potential RNA substrate recognition site in VSV methlyase and determined its role in mRNA cap methylation. We identified two aromatic amino acid residues that are essential for both G-N-7 and 2'-O methylation and may play a critical role in the stacking interaction with mRNA cap. Clearly, unraveling of the crystal structure of VSV MTase will provide more mechanistic insight to this unusual mRNA cap methylation. We also showed that mutations to the putative RNA substrate recognition site significantly diminished viral replication. These findings suggest that mRNA cap methylation is an attractive antiviral target for NNS RNA viruses.

Materials and methods

Plasmid construction and site-directed mutagenesis

Plasmids encoding VSV N (pN), P(pP), and L (pL) genes, and an infectious cDNA clone of the viral genome, pVSV1(+), were generous gifts from Dr. Gail Wertz (Whelan et al., 1995). Using pVSV1(+) as a template, the coding sequence in the *L* gene was modified by site-directed mutagenesis using the QuikChange methodology (Stratagene, La Jolla, CA). The presence of the desired mutation was confirmed by sequence analysis of a 2-kb region of pVSV1(+) that spanned from *Fse*I site to an *Hin*dIII site. The pVSV1(+) variants were digested with *Fse*I and *Hin*dIII, and the resulting 2-kb fragment was subcloned back into pVSV1(+) at the same sites. This approach ensured that no other sequence alterations were introduced during the mutagenesis reaction. Using this method, a total of sixteen *L* gene mutations was generated.

Recovery and purification of recombinant VSV

Recovery of recombinant VSV from the infectious clone was performed essentially as described previously (Whelan et al., 1995). Briefly, recombinant VSV was recovered by co-transfection of pVSV (+), pN, pP, and pL into BSRT7 cells infected with a recombinant vaccinia virus (vTF7-3) expressing T7 RNA polymerase (Fuerst et al., 1986). At 96 h posttransfection, cell culture fluids were collected, filtered through 0.2 μM filter, and recombinant virus was further amplified in BSRT7 cells. Subsequently, the viruses were plaque purified. Viral plaque assay was performed in Vero cells as described previously (Whelan et al., 1995). Individual plaques were isolated, and seed stocks were amplified on BSRT7 cells. To generate large stocks, plaque purified viruses were inoculated into 10 confluent T150 flask BSRT7 cells at a multiplicity of infection (MOI) of 0.01 in a volume of 2 ml of Dulbecco modified Eagle medium (DMEM). At 1 h postadsorption, 15 ml of DMEM (supplemented with 2% fetal bovine serum) was added to the cultures, and infected cells were incubated at 37 °C for 24 to 48 h. Cell culture fluids were harvested when extensive cytopathic effect (CPE) was observed. Cell culture fluids were clarified by centrifugation at 3,000×*g* for 10 min. Virus was concentrated by centrifugation at 40,000×*g* for 90 min at 4 °C in a Ty 50.2 rotor. The pellet was resuspended in NTE buffer (100 mM NaCl, 10 mM Tris, 1 mM EDTA [pH 7.4]) and further purified through 10% sucrose NTE by centrifugation at 150,000*g* for 1 h at 4 °C in an SW50.1 rotor. The final pellet was resuspended in 0.3 ml of NTE buffer. The virus titer was determined by plaque assay in Vero cells, and the protein content was measured by the Bradford assay (Sigma Chemical Co., St. Louis, MO). The *L* genes of the purified viruses were sequenced again, and these stocks were used for in vitro transcription reactions.

Single-cycle growth curves

Confluent BSRT-7 cells were either infected with individual viruses at an MOI of 3 or infected with 20 $TCID_{50}$ of viruses. After 1 h of adsorption, the inoculum was removed, the cells were washed twice with DMEM, fresh DMEM (supplemented with 2% fetal bovine serum) was added, and infected cells were incubated at 37 °C. Aliquots of the cell culture fluid were removed at the indicated intervals, and virus

titers were determined by plaque assay in Vero cells or a $TCID_{50}$ assay using Reed–Muench method in BSRT7 cells (Reed and Muench, 1938).

Transcription of viral RNA in vitro

Viral RNA was synthesized in vitro essentially as described previously (Baltimore et al., 1970; Ball and White, 1976; Li et al., 2005, 2006, 2007). 20 μg of purified recombinant VSV was activated by incubation with detergent for 5 min at room temperature. RNA synthesis reactions were performed in the presence of nucleoside triphosphates (1 mM ATP and 0.5 mM each of CTP, GTP, and UTP) and actinomycin D. Where indicated, reactions were supplemented with 1 mM SAM or *S*-adenosylhomocysteine (SAH) or with 15 μCi of [α-^{32}P]GTP (3,000 Ci/mmol) or 15 μCi of [^{3}H]SAM (85 Ci/mmol; Perkin-Elmer, Wellesley, MA). After incubation at 30 °C for 5 h, total RNA was purified by RNeasy purification kit (Qiagen). Purified RNA was analyzed by electrophoresis on acid-agarose gels as described previously (Li et al, 2005), and the products were detected by phosphoimage analysis.

Analysis of mRNA cap methyltransferase

For G-N-7 MTase assay, in vitro transcription reactions were performed in the presence of 15 μCi of [α-^{32}P]GTP and 1 mM SAM or SAH. The RNAs were purified and digested with 2U of tobacco acid pyrophosphatase (TAP; Epicenter, Madison, WI) and the products were resolved by thin-layer chromatography (TLC) on PEI-F cellulose sheets (EM Biosciences). For the ribose-2'-O MTase assay, in vitro transcription reactions were performed in the presence of 15 μCi of [^{3}H]SAM. The purified RNAs were digested with 5U of nuclease P1 (Sigma) or double digested by 10 U of RNase T2 and 2 U of TAP, and the products were spotted onto a TLC plate. The TLC plate was developed using 1.2 M $LiCl_2$, dried in 70 °C incubator, and the radioactive spots were detected by using a phosphorimager (GE Healthcare, Typhoon). Markers 7^{m}GpppA and GpppA were purchased from New England Biolabs, and GpppA^{m} and 7^{m}GpppA^{m} were purchased from P-L Biochemicals. Marker 7^{m}Gp and Gp were generated by TAP digestion of 7^{m}GpppA and GpppA. All the markers were visualized by UV shadowing at 254 nm.

Primer extension assays

A primer extension assay was used to quantify the amount of mRNA synthesized in vitro (Li et al., 2006, 2007). Briefly, a minus sense oligonucleotide, nucleotides 130–115 of the VSV genome, was end-labeled using [γ-^{32}P]ATP and T4 polynucleotide kinase (Invitrogen). The labeled primer was purified, and 7.5 pmol was annealed with 1/25 of the total RNA from an in vitro transcription reaction and extended by Superscript III reverse transcriptase (Invitrogen) at 50 °C. Products were analyzed by electrophoresis on denaturing 6% polyacrylamide gels and detected by phosphoimage analysis.

Scintillation counting

To further analyze mRNA cap methylation, aliquots of purified RNA from [^{3}H] SAM experiments were mixed with 4 ml of ReadySafe scintillation mixture (Beckman Coulter), and dpm were measured by using a TriCarb Model 314X liquid scintillation counter (Packard Instrument Company).

Quantitative and statistical analysis

Quantitative analysis was performed by either densitometric scanning of autoradiographs or by using a phosphorimager (GE Healthcare, Typhoon) and ImageQuant TL software (GE Healthcare, Piscataway, NJ). Each experiment was done three to six times. Statistical analysis was performed by a paired Student's *t* test. A value of $p<0.05$ was considered statistically significant.

Acknowledgments

We thank Gail Wertz for her generous gift of VSV infectious clone. We thank Lijun Liu for structural modeling of VSV MTase. We thank Sean Whelan, Ronald Iorio, and Ashley Predmore for critical reviews of the manuscript. X. Z. was supported by a fellowship from Zhejiang University, China. Part of this study was supported by a grant (2010-65119-20602) from the USDA Agricultural and Food Research Initiative to J. L.

References

Abraham, G., Banerjee, A.K., 1976. Sequential transcription of the genes of vesicular stomatitis virus. Proc. Natl. Acad. Sci. U. S. A. 73 (5), 1504–1508.
Abraham, G., Rhodes, D.P., Banerjee, A.K., 1975. The 5' terminal structure of the methylated mRNA synthesized in vitro by vesicular stomatitis virus. Cell 5 (1), 51–58.
Ball, L.A., White, C.N., 1976. Order of transcription of genes of vesicular stomatitis virus. Proc. Natl. Acad. Sci. U. S. A. 73 (2), 442–446.
Baltimore, D., Huang, A.S., Stampfer, M., 1970. Ribonucleic acid synthesis of vesicular stomatitis virus. II. An RNA polymerase in the virion. Proc. Natl. Acad. Sci. U. S. A. 66 (2), 572–576.
Barbosa, E., Moss, B., 1978. mRNA(nucleoside-2'-)-methyltransferase from vaccinia virus. Characteristics and substrate specificity. J. Biol. Chem. 253 (21), 7698–7702.
Bugl, H., Fauman, E.B., Staker, B.L., Zheng, F., Kushner, S.R., Saper, M.A., Bardwell, J.C., Jakob, U., 2000. RNA methylation under heat shock control. Mol. Cell 6 (2), 349–360.
Bujnicki, J.M., Rychlewski, L., 2002. In silico identification, structure prediction and phylogenetic analysis of the 2'-O-ribose (cap 1) methyltransferase domain in the large structural protein of ssRNA negative-strand viruses. Protein Eng. 15 (2), 101–108.
Cowling, V.H., 2010. Regulation of mRNA cap methylation. Biochem. J. 425 (2), 295–302.
De la Pena, M., Kyrieleis, O.J., Cusack, S., 2007. Structural insights into the mechanism and evolution of the vaccinia virus mRNA cap N7 methyl-transferase. EMBO J. 26 (23), 4913–4925.
Decroly, E., Imbert, I., Coutard, B., Bouvet, M., Selisko, B., Alvarez, K., Gorbalenya, A.E., Snijder, E.J., Canard, B., 2008. Coronavirus nonstructural protein 16 is a cap-0 binding enzyme possessing (nucleoside-2'O)-methyltransferase activity. J. Virol. 82 (16), 8071–8084.
Dong, H., Ray, D., Ren, S., Zhang, B., Puig-Basagoiti, F., Takagi, Y., Ho, C.K., Li, H., Shi, P.Y., 2007. Distinct RNA elements confer specificity to flavivirus RNA cap methylation events. J. Virol. 81 (9), 4412–4421.
Dong, H., Ren, S., Zhang, B., Zhou, Y., Puig-Basagoiti, F., Li, H., Shi, P.Y., 2008. West Nile virus methyltransferase catalyzes two methylations of the viral RNA cap through a substrate-repositioning mechanism. J. Virol. 82 (9), 4295–4307.
Egloff, M.P., Benarroch, D., Selisko, B., Romette, J.L., Canard, B., 2002. An RNA cap (nucleoside-2'-O-)-methyltransferase in the flavivirus RNA polymerase NS5: crystal structure and functional characterization. EMBO J. 21 (11), 2757–2768.
Emerson, S.U., Wagner, R.R., 1972. Dissociation and reconstitution of the transcriptase and template activities of vesicular stomatitis B and T virions. J. Virol. 10, 297–309.
Emerson, S.U., Yu, Y., 1975. Both NS and L proteins are required for in vitro RNA synthesis by vesicular stomatitis virus. J. Virol. 15, 1348–1356.
Fabrega, C., Hausmann, S., Shen, V., Shuman, S., Lima, C.D., 2004. Structure and mechanism of mRNA cap (guanine-N7) methyltransferase. Mol. Cell 13, 77–89.
Ferron, F., Longhi, S., Henrissat, B., Canard, B., 2002. Viral RNA-polymerases—a predicted 2'-O-ribose methyltransferase domain shared by all Mononegavirales. Trends. Biochem. Sci. 27 (5), 222–224.
Fuerst, T.R., Niles, E.G., Studier, F.W., Moss, B., 1986. Eukaryotic transient-expression system based on recombinant vaccinia virus that synthesizes bacteriophage T7 RNA polymerase. Proc. Natl. Acad. Sci. U. S. A. 83 (21), 8122–8126.
Furuichi, Y., Shatkin, A.J., 2000. Viral and cellular mRNA capping: past and prospects. Adv. Virus. Res. 55, 135–184.
Furuichi, Y., LaFiandra, A., Shatkin, A.J., 1977. 5'-Terminal structure and mRNA stability. Nature 266 (5599), 235–239.
Galloway, S.E., Wertz, G.W., 2008. S-adenosyl homocysteine-induced hyperpolyadenylation of vesicular stomatitis virus mRNA requires the methyltransferase activity of L protein. J. Virol. 82 (24), 12280–12290.
Galloway, S.E., Richardson, P.E., Wertz, G.W., 2008. Analysis of a structural homology model of the 2'-O-ribose methyltransferase domain within the vesicular stomatitis virus L protein. Virology 382 (1), 69–82.
Grdzelishvili, V.Z., Smallwood, S., Tower, D., Hall, R.L., Hunt, D.M., Moyer, S.A., 2005. A single amino acid change in the L-polymerase protein of vesicular stomatitis virus completely abolishes viral mRNA cap methylation. J. Virol. 79 (12), 7327–7337.
Hager, J., Staker, B.L., Bugl, H., Jakob, U., 2002. Active site in RrmJ, a heat shock-induced methyltransferase. J. Biol. Chem. 277 (44), 41978–41986.
Hager, J., Staker, B.L., Jakob, U., 2004. Substrate binding analysis of the 23S rRNA methyltransferase RrmJ. J. Bacteriol. 186 (19), 6634–6642.

Hercyk, N., Horikami, S.M., Moyer, S.A., 1988. The vesicular stomatitis virus L protein possesses the mRNA methyltransferase activities. Virology 163 (1), 222–225.
Hodel, A.E., Gershon, P.D., Shi, X., Quiocho, F.A., 1996. The 1.85 A structure of vaccinia protein VP39: a bifunctional enzyme that participates in the modification of both mRNA ends. Cell 85 (2), 247–256.
Hodel, A.E., Gershon, P.D., Quiocho, F.A., 1998. Structural basis for sequence-nonspecific recognition of 5'-capped mRNA by a cap-modifying enzyme. Mol. Cell 1, 443–447.
Hu, G., Gershon, P.D., Hodel, A.E., Quiocho, F.A., 1999. mRNA cap recognition: dominant role of enhanced stacking interactions between methylated bases and protein aromatic side chains. Proc. Natl. Acad. Sci. U. S. A. 96 (13), 7149–7154.
Issur, M., Geiss, B.J., Bougie, I., Picard-Jean, F., Despins, S., Mayette, J., Hobdey, S.E., Bisaillon, M., 2009. The flavivirus NS5 protein is a true RNA guanylyltransferase that catalyzes a two-step reaction to form the RNA cap structure. RNA 15 (12), 2340–2350.
Iverson, L.E., Rose, J.K., 1981. Localized attenuation and discontinuous synthesis during vesicular stomatitis virus transcription. Cell 23 (2), 477–484.
Koonin, E., Moss, B., 2010. Viruses know more than one way to don a cap. Proc. Natl. Acad. Sci. U. S. A. 107 (8), 3283.
Li, C., Xia, Y., Gao, X., Gershon, P., 2004. Mechanism of RNA 2-O-methylation: evidence that the catalytic lysine acts to steer rather than deprotonate the target nucleophile. Biochemistry 43 (19), 5680–5687.
Li, J., Fontaine-Rodriguez, E.C., Whelan, S.P., 2005. Amino acid residues within conserved domain VI of the vesicular stomatitis virus large polymerase protein essential for mRNA cap methyltransferase activity. J. Virol. 79 (21), 13373–13384.
Li, J., Wang, J.T., Whelan, S.P., 2006. A unique strategy for mRNA cap methylation used by vesicular stomatitis virus. Proc. Natl. Acad. Sci. U. S. A. 103 (22), 8493–8498.
Li, J., Chorba, J.S., Whelan, S.P., 2007. Vesicular stomatitis viruses resistant to the methylase inhibitor sinefungin upregulate RNA synthesis and reveal mutations that affect mRNA cap methylation. J. Virol. 81 (8), 4104–4115.
Li, J., Rahmeh, A., Morelli, M., Whelan, S.P., 2008. A conserved motif in region V of the large polymerase proteins of nonsegmented negative-sense RNA viruses that is essential for mRNA capping. J. Virol. 82 (2), 775–784.
Li, J., Rahmeh, A., Brusic, V., Whelan, S.P., 2009. Opposing effects of inhibiting cap addition and cap methylation on polyadenylation during vesicular stomatitis virus mRNA synthesis. J. Virol. 83 (4), 1930–1940.
Lockless, S.W., Cheng, H.T., Hodel, A.E., Quiocho, F.A., Gershon, P.D., 1998. Recognition of capped RNA substrates by VP39, the vaccinia virus-encoded mRNA cap-specific 2'-O-methyltransferase. Biochemistry 37 (23), 8564–8574.
Marcotrigiano, J., Gingras, A.C., Sonenberg, N., Burley, S.K., 1997. Cocrystal structure of the messenger RNA 5' cap-binding protein (eIF4E) bound to 7-methyl-GDP. Cell 89 (6), 951–961.
Moyer, S.A., 1981. Alteration of the 5' terminal caps of the mRNAs of vesicular stomatitis virus by cycloleucine in vivo. Virology 112 (1), 157–168.
Ogino, T., Banerjee, A.K., 2007. Unconventional mechanism of mRNA capping by the RNA-dependent RNA polymerase of vesicular stomatitis virus. Mol. Cell 25 (1), 85–97.
Ogino, T., Banerjee, A.K., 2010. The HR motif in the RNA-dependent RNA polymerase L protein of Chandipura virus is required for unconventional mRNA-capping activity. J. Gen. Virol. 91, 1311–1314.
Ogino, T., Yadav, S.P., Banerjee, A.K., 2010. Histidine-mediated RNA transfer to GDP for unique mRNA capping by vesicular stomatitis virus RNA polymerase. Proc. Natl. Acad. Sci. U. S. A. 107 (8), 3463–3468.
Poch, O., Blumberg, B.M., Bougueleret, L., Tordo, N., 1990. Sequence comparison of five polymerases (L proteins) of unsegmented negative-strand RNA viruses: theoretical assignment of functional domains. J. Gen. Virol. 71 (Pt 5), 1153–1162.
Quiocho, F.A., Hu, G., Gershon, P.D., 2000. Structural basis of mRNA cap recognition by proteins. Curr. Opin. Struct. Biol. 10 (1), 78–86.
Rahmeh, A.A., Li, J., Kranzusch, P.J., Whelan, S.P., 2009. Ribose 2'-O methylation of the vesicular stomatitis virus mRNA cap precedes and facilitates subsequent guanine-N-7 methylation by the large polymerase protein. J. Virol. 83 (21), 11043–11050.
Ray, D., Shah, A., Tilgner, M., Guo, Y., Zhao, Y., Dong, H., Deas, T.S., Zhou, Y., Li, H., Shi, P.Y., 2006. West Nile virus 5'-cap structure is formed by sequential guanine N-7 and ribose 2'-O methylations by nonstructural protein 5. J. Virol. 80 (17), 8362–8370.
Reed, L.J., Muench, H., 1938. A simple method of estimating fifty percent endpoints. Am. J. Epidemiol. 27, 493–497.
Reinisch, K.M., Nibert, M.L., Harrison, S.C., 2000. Structure of the reovirus core at 3.6 A resolution. Nature 404 (6781), 960–967.
Rose, J.K., Whitt, M.A., 2001. Rhabdoviridae: the viruses and their replication, In: Knipe, D.M., Howley, P.M. (Eds.), Fundamental Virology, 4th ed. Lippincott Williams and Wilkins, Philadelphia, pp. 665–688.
Schluckebier, G., O'Gara, M., Saenger, W., Cheng, X., 1995. Universal catalytic domain structure of AdoMet-dependent methyltransferases. J. Mol. Biol. 247 (1), 16–20.
Shuman, S., 2001. Structure, mechanism, and evolution of the mRNA capping apparatus. Prog. Nucleic. Acid. Res. Mol. Biol. 66, 1–40.
Shuman, S., Schwer, B., 1995. RNA capping enzyme and DNA ligase: a superfamily of covalent nucleotidyl transferases. Mol. Microbiol. 17 (3), 405–410.
Villarreal, L.P., Breindl, M., Holland, J.J., 1976. Determination of molar ratios of vesicular stomatitis virus induced RNA species in BHK21 cells. Biochemistry 15, 1663–1667.
Wang, J.T., McElvain, L.E., Whelan, S.P., 2007. Vesicular stomatitis virus mRNA capping machinery requires specific cis-acting signals in the RNA. J. Virol. 81 (20), 11499–11506.
Whelan, S.P., Ball, L.A., Barr, J.N., Wertz, G.T., 1995. Efficient recovery of infectious vesicular stomatitis virus entirely from cDNA clones. Proc. Natl. Acad. Sci. U. S. A. 92 (18), 8388–8392.
Whelan, S.P., Barr, J.N., Wertz, G.W., 2004. Transcription and replication of nonsegmented negative-strand RNA viruses. Curr. Top. Microbiol. Immunol. 283, 61–119.
Zheng, S., Shuman, S., 2008a. Mutational analysis of vaccinia virus mRNA cap (guanine-N7) methyltransferase reveals essential contributions of the N-terminal peptide that closes over the active site. RNA 14 (11), 2297–2304.
Zheng, S., Shuman, S., 2008b. Structure-function analysis of vaccinia virus mRNA cap (guanine-N7) methyltransferase. RNA 14 (4), 696–705.
Zhou, Y., Ray, D., Zhao, Y., Dong, H., Ren, S., Li, Z., Guo, Y., Bernard, K.A., Shi, P.Y., Li, H., 2007. Structure and function of flavivirus NS5 methyltransferase. J. Virol. 81 (8), 3891–3903.